

# HOT3D: Hand and Object Tracking in 3D from Egocentric Multi-View Videos

Prithviraj Banerjee, Sindi Shkodrani, Pierre Moulon, Shreyas Hampali, Shangchen Han,  
Fan Zhang, Linguang Zhang, Jade Fountain, Edward Miller, Selen Basol,  
Richard Newcombe, Robert Wang, Jakob Julian Engel, Tomas Hodan

Meta Reality Labs [facebookresearch.github.io/hot3d](https://facebookresearch.github.io/hot3d)

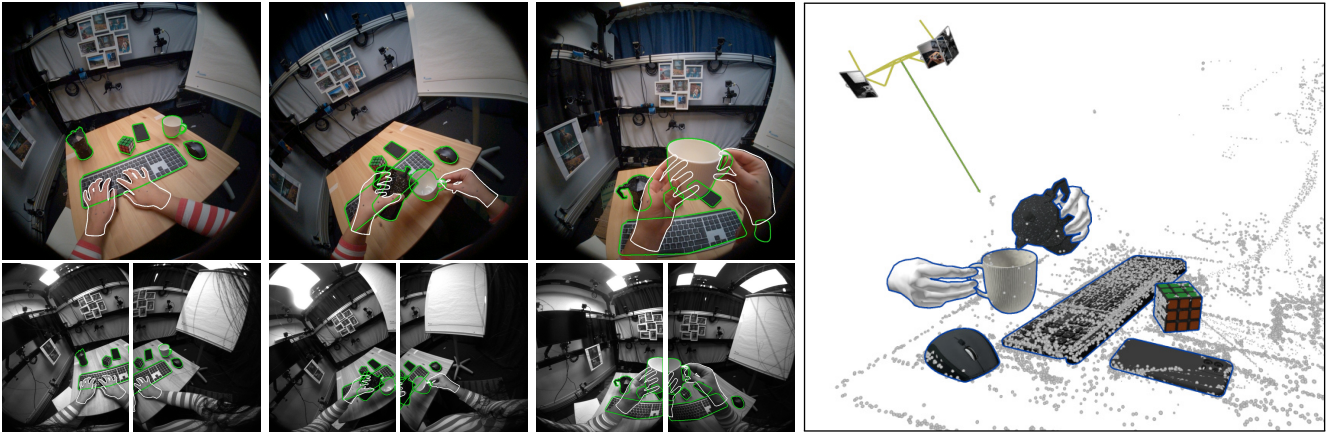


Figure 1. **HOT3D overview.** The dataset includes multi-view egocentric image streams from Aria [13] and Quest 3 [41] annotated with high-quality ground-truth 3D poses and models of hands and objects. Three multi-view frames from Aria are shown on the left, with contours of 3D models of hands and objects in the ground-truth poses in white and green, respectively. Aria also provides 3D point clouds from SLAM and eye gaze information (right).

## Abstract

We introduce *HOT3D*, a publicly available dataset for egocentric hand and object tracking in 3D. The dataset offers over 833 minutes (more than 3.7M images) of multi-view RGB/monochrome image streams showing 19 subjects interacting with 33 diverse rigid objects, multi-modal signals such as eye gaze or scene point clouds, as well as comprehensive ground-truth annotations including 3D poses of objects, hands, and cameras, and 3D models of hands and objects. In addition to simple pick-up/observe/put-down actions, *HOT3D* contains scenarios resembling typical actions in a kitchen, office, and living room environment. The dataset is recorded by two head-mounted devices from Meta: Project Aria, a research prototype of light-weight AR/AI glasses, and Quest 3, a production VR headset sold in millions of units. Ground-truth poses were obtained by a professional motion-capture system using small optical markers attached to hands and objects. Hand annotations are provided in the *UmeTrack* and *MANO* formats and objects are represented by 3D meshes with PBR materials obtained by an in-house scanner. In our experiments, we demonstrate the effectiveness of multi-view egocentric data for three popular tasks: 3D hand tracking, 6DoF object pose estimation, and 3D lifting of unknown in-hand objects. The evaluated multi-view methods, whose benchmarking is uniquely enabled by *HOT3D*, significantly outperform their single-view counterparts.

## 1. Introduction

We use our hands to communicate, interact with objects, or utilize objects as tools to act upon our environment. The dexterity with which we can manipulate objects is unmatched by other species and has been a key factor in our evolution [2]. Hand-object interaction has therefore naturally received considerable attention from various research fields, including computer vision [48].

A vision-based system for automatic understanding of hand-object interaction, which would be able to capture information about 3D motion, shape and contact of hands and objects, would be useful for a wide range of applications. For instance, such a system could enable transferring manual skills between users by first capturing expert users performing a sequence of hand-object interactions (while assembling a piece of furniture, doing a tennis serve, etc.), and later using the captured information to guide less experienced users, e.g., via AR glasses. The skills could be similarly transferred from humans to robots. Such a system could also help AI assistants better understand the context of a user’s actions, or enable new input capabilities for AR/VR users. For example, it could turn any physical surface into a virtual keyboard or transform any pencil into a multi-functional magic wand. However, the accuracy and speed of existing methods for understanding hand-object interaction are not sufficient to reliably support such applications.

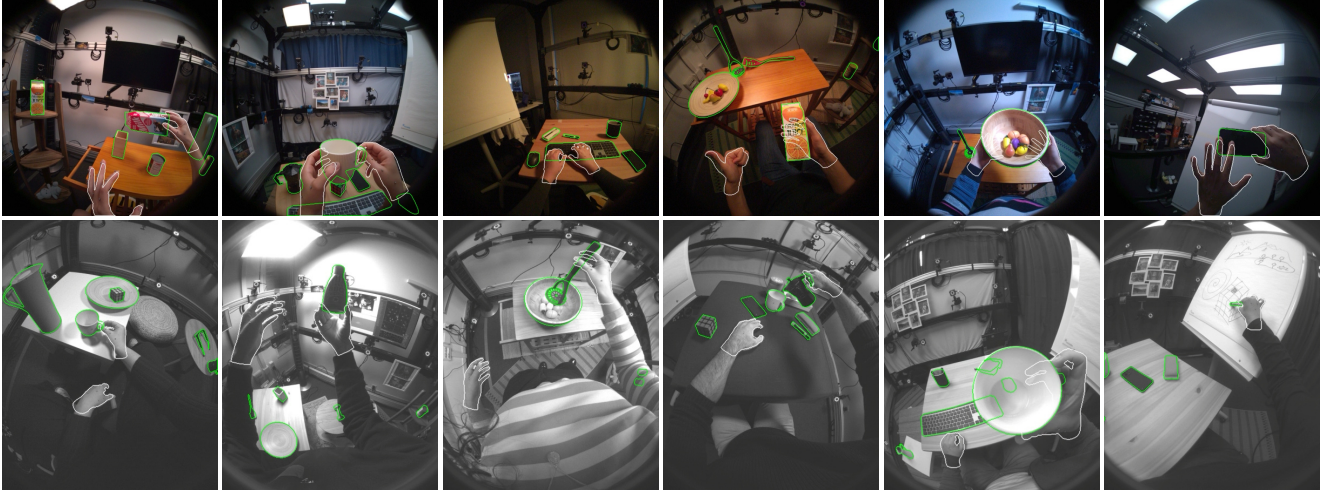


Figure 2. **Sample images from Aria (top) and Quest 3 (bottom).** Aria recordings include one RGB and two monochrome image streams, while Quest 3 recordings include two monochrome streams – only images from one of the multi-view streams are shown. Contours of 3D models of hands and objects in the ground-truth poses are shown in white and green respectively. In addition to simple pick-up/observe/put-down actions, the subjects perform actions that are common in a kitchen, office, and living room. To increase diversity, the lighting, furniture, and decorations in the capture lab were regularly randomized.

To accelerate computer vision research on hand-object interaction, we are publicly releasing HOT3D, an egocentric dataset for training and evaluating methods for hand and object tracking in 3D. The dataset is recorded using two recent head-mounted devices from Meta: Project Aria [13], which is a research prototype of light-weight AI glasses, and Quest 3 [41], a virtual-reality headset that has shipped millions of units. The dataset offers over 833 minutes of egocentric video streams, which include over 1.5M multi-view frames (over 3.7M images) and show 19 subjects interacting with 33 diverse rigid objects. Besides a simple inspection scenario, where subjects pick up, observe, and put down the objects, the sequences show scenarios resembling typical actions in kitchen, office, and living room spaces. Hands and objects are annotated with accurate 3D poses collected using a passive marker-based motion-capture system. The dataset also includes 3D object models which were obtained by an in-house scanning-based 3D object reconstruction pipeline and include high-resolution geometry and PBR materials [40]. Recordings from Aria additionally include 3D scene point clouds from SLAM and eye gaze information. Sample images are in Fig. 2.

The HOT3D dataset is primarily intended for training and evaluation of hand and object tracking methods *in 3D space* from *localized, egocentric, multi-view video streams*, as opposed to monocular views or individual images. Since images from all streams are synchronized with a hardware trigger (*i.e.*, captured at the same timestamp), the dataset enables development of methods that can leverage multi-view and/or temporal information. While providing a testbed for CAD-based object tracking, the dataset also enables a CAD-free tracking setup by providing reference sequences showing different views at each object, which can be used to onboard the objects in a few-shot manner. Furthermore, the dataset can be used for tasks such as 3D object reconstruction and 2D detection or segmentation of hand-object interactions. We also

encourage research that leverages the eye gaze information from Aria, which can enable predicting the user’s intent, or efficient allocation of the computational budget via foveated sensing.

To analyze the effectiveness of multi-view egocentric data, we present experiments showing that multi-view methods significantly outperform their single-view variants. In addition to multi-view 3D object tracking, we focused on the tasks of multi-view 6DoF pose estimation of unseen objects and 3D lifting of in-hand objects [51], for which we developed strong baselines. Our results highlight the advantages of multi-view and temporal data, which is under-explored in hand/object tracking research due to limited datasets.

In summary, we make the following contributions:

1. **Publicly available HOT3D dataset:** We collected and release the first large-scale dataset that offers (1) multi-view egocentric video streams recorded with real headsets, (2) high-quality pose annotations of the headset and multiple objects in each scene, as well as pose and shape annotations of both hands, (3) non-trivial hand-object interaction scenarios with dynamic grasps, and (4) 3D object models with materials for physically based rendering. HOT3D enables benchmarking methods for various 2D/3D tasks on understanding hand-object interaction.
2. **Strong baselines for tasks enabled by HOT3D:** We developed simple yet powerful multi-view baselines for two increasingly popular tasks that are relevant for augmented/mixed reality: 6DoF pose estimation of objects with known 3D models (extending FoundPose [50]), and 3D lifting of unknown in-hand objects (based on stereo matching of DINOv2 [49] features). Source code of the methods will be publicly available.
3. **Demonstrated effectiveness of multi-view egocentric data:** Our experiments show that multi-view methods for 3D hand tracking, 6DoF object pose estimation, and 3D lifting of hand-

Dataset	Images	Channels	Ego / exo	HW trigger	Headsets	Subjects	Hands	Objects	..per scene	Gaze	Annotation
HOT3D (ours)	3.7M	RGB/gray	2-3 / 0	✓	Aria, Quest 3	19	Both	33	~6	✓	Mocap
ARTIC [15]	2.1M	RGB	1 / 8	✓	Helmet	10	Both	11	1	✗	Mocap
HOI4D [39]	2.4M	RGB-D	2 / 0	✗	Helmet	4	Both	800	1-12	✗	RGB-D + man.
ENIGMA-51 [52]	45K	RGB	1 / 0	-	HoloLens 2	19	Both	25	25	✗	Manual
DexYCB [8]	582K	RGB-D	0 / 8	✓	-	10	Single	20	2-4	✗	Manual
HOCAP [69]	699K	RGB-D	1 / 9	✗	Hololens	9	Both	64	4	✗	RGB-D + optim.
HOGraspNet [9]	1.5M	RGB-D	0 / 4	✓	-	99	Single	30	1	✗	RGB-D + optim.
H2O-3D [24]	75K	RGB-D	0 / 5	✗	-	6	Both	10	1	✗	RGB-D + optim.
HO-3D [23]	78K	RGB	0 / 1	-	-	10	Single	10	~6	✗	RGB-D + optim.
H2O [38]	572K	RGB-D	1 / 4	✓	Helmet	4	Both	8	1	✗	RGB-D + optim.
ContactPose [5]	2.9M	RGB-D	0 / 3	✗	-	50	Both	25	1	✗	RGB-D + mocap
ObMan [27]	147K	Synth. RGB	0 / 1	-	-	20	Single	2772	1	✗	Synthetic

Table 1. **Datasets with 3D hands and object annotations.** HOT3D is the first dataset to provide multi-view, hardware time-synced egocentric videos captured with real headsets. It is the largest dataset in terms of total image count and provides high quality ground-truth annotations (comparable to [15]).

held objects clearly outperform their single-view counterparts. This is an important result for research on power-efficient egocentric vision systems, which can typically afford a multi-view camera setup [13] but not *e.g.*, active depth sensors [68].

## 2. Related work

The progress of research in computer vision has been strongly influenced by benchmark datasets [14, 19, 32, 57, 58] which enable comparing of methods and understanding of their limitations. In this section, we first review existing datasets with either hand or object pose annotations, and then focus on datasets that offer annotations of hands and hand-manipulated objects.

**Datasets with hands only.** Vision-based 3D hand pose estimation and tracking has been extensively studied for many years, with the first methods focusing on custom datasets with monochrome images [29, 54]. Significant improvements in pose accuracy were later achieved on RGB-D images from datasets such as NYU [66], ICVL [65], MSRA [63], Tzionas *et al.* [67], EgoDexter [44], or HANDS17 [73]. Recently, partly motivated by AR/VR use cases where depth sensors are often unavailable due to high power consumption, the research community has largely switched to RGB or monochrome images, working on datasets such as the Stereo dataset [74], InterHand2.6M [43], FreiHAND [76], UmeTrack [26], AssemblyHands [47], and datasets with pose annotations of both hands and objects reviewed below.

**Datasets with objects only.** Research on 6DoF object pose estimation and tracking has followed a similar path, starting off with custom monochrome datasets [45, 55] and later largely switching to RGB-D datasets such as LM [30], YCB-V [71], and T-LESS [31], which are included in the BOP benchmark [32-34, 64]. The benchmark currently includes twelve datasets in a unified format, offering 3D object models and training and test RGB-D images annotated with 6DoF object poses. The 3D object models are created manually or using KinectFusion-like systems [46] for 3D surface reconstruction. The training images are real or synthetic (photo-realistically rendered with BlenderProc [11, 12]) and all test images are real. Besides these instance-level datasets, the community also uses category-level RGB-D datasets such as Wild6D [17],

HouseCat6D [36], and PhoCal [70]. Recent methods started to focus again on estimating object pose from RGB-only images, using datasets such as OnePose [62] and HANDAL [21].

**Datasets with hands and objects.** Many existing datasets include images of hands and objects (*e.g.*, [1, 6, 10, 16, 60, 75]), but only provide annotations in the form of 2D bounding boxes, segmentation masks, or action labels. Some datasets for 3D hand pose estimation (*e.g.*, [44, 47, 76]) include images of hands interacting with objects, but do not provide 6DoF object pose annotations.

The first dataset with ground-truth poses of both hands and objects was created by Sridhar *et al.* [61] and offers 3014 exocentric RGB-D images of a hand manipulating a cube, manually annotated with fingertip positions and 6DoF poses of the cube. To avoid the manual annotation, which is tedious and not scalable, the FHPA dataset [18] used magnetic sensors attached to one hand and objects, noticeably affecting their appearance. This dataset includes 105K egocentric RGB-D images with ground-truth poses of a single hand and 4 objects. The ObMan dataset [27] resorted to synthesizing images of hands grasping objects, with the grasps generated by an algorithm from robotics.

HO-3D [23] was the first dataset with real images annotated by an optimization procedure that leverages multi-view RGB-D image streams and is almost fully automatic. The dataset offers 78K images from several exocentric cameras, showing 10 subjects and 10 objects. A similar annotation procedure was used for several subsequent datasets [3, 8, 24, 38, 39]. H2O [38] includes 572K egocentric multi-view RGB-D images of 4 subjects manipulating 8 objects. H2O-3D [24] provides 75K exocentric RGB images of 6 subjects manipulating 10 YCB objects [7]. DexYCB [8] consists of 1000 clips of 3 seconds with the total of 582K RGB-D images, recorded from 8 exocentric views and showing 10 subjects picking up 20 YCB objects with near-static grasps. HOI4D [39] includes 2.4M egocentric RGB-D images from over 4000 video sequences showing 9 subjects interacting with 800 different objects from 16 categories in 610 different indoor environments. Besides rigid objects, this dataset contains articulated objects, but focuses on simpler scenarios with a single hand and a single object, and only includes single-view video sequences. An RGB-D optimization procedure was also used in



ContactPose [5] along with the information from thermal cameras for accurately annotating hand poses, while the object poses were annotated using optical markers. ContactPose includes 2.9M RGB-D images of 50 subjects grasping 25 household objects, however, the grasps are static, background green and all objects are blue (3D printed), which makes the images less realistic.

Similar to HOT3D, ground-truth poses of hands and objects in the recent ARCTIC dataset [15] were collected with a marker-based motion-capture system. This dataset includes 2.1M RGB images showing 10 subjects interacting with 11 articulated objects. The images were captured at 233K timestamps from 9 views, only one of which is egocentric (recorded with a mock-up of an egocentric device – a camera mounted on a helmet).

### 3. HOT3D dataset

**833 minutes of recordings.** The HOT3D dataset includes egocentric, multi-view, synchronized data streams recorded with Project Aria [13] and Quest 3 [41]. Image streams contain 1.5M multi-view frames consisting of 3.7M images. Each frame from Aria consists of one RGB 1408×1408 image and two monochrome 640×480 images. Each frame from Quest 3 consists of two monochrome 1280×1024 images. Intrinsic camera parameters and camera-to-world transformations are available for all images. All streams were recorded at 30 fps. Every recording from Aria also includes a 3D point cloud of the scene (from SLAM) and per-frame eye gaze information. See supplement for more details about Aria and Quest 3.

**3D mesh models of 33 objects.** The models were obtained using an in-house scanning-based 3D object reconstruction pipeline, which provides high-resolution geometry and PBR [40] materials. These materials include metallic, roughness, and normal maps and enable rendering of photo-realistic training images [33, 35]. The object collection includes household and office objects of diverse appearance, size, and affordances (Fig. 3).

**19 diverse subjects.** To ensure diversity, we recruited 19 participants with different hand appearances and shapes. Hands of each participant were scanned by a custom 3D hand scanner and are provided in the UmeTrack [26] and MANO [56] formats.

**4 everyday scenarios.** Besides a simple inspection scenario, where subjects pick up, observe, and put down objects, subjects were asked to perform typical actions in a kitchen, office, and living room. All scenarios were captured in the same lab equipped with scenario-specific furniture. In each recording, subjects were asked to interact with up to 6 objects. To enhance diversity within the dataset, we regularly randomized various aspects such as lighting, furniture placement, and decorative elements. The resulting dataset consists of 425 recordings, with 199 captured using Aria and 226 using Quest 3. Each recording is around 2 minutes long.

**Ground-truth annotations.** Recordings are annotated with per-frame ground-truth poses of hands and objects obtained in a motion-capture lab shown in Fig. 5 and described in the supplement. Object and wrist poses are represented as 3D rigid trans-



Figure 3. **High-quality 3D mesh models.** This image shows a rendering of the 33 object models, demonstrating their quality. The models were obtained by an in-house scanning-based 3D object reconstruction pipeline and include PBR materials, which enable rendering of photo-realistic training images for methods that require it. The collection includes household and office objects of diverse appearance, size, and affordances.

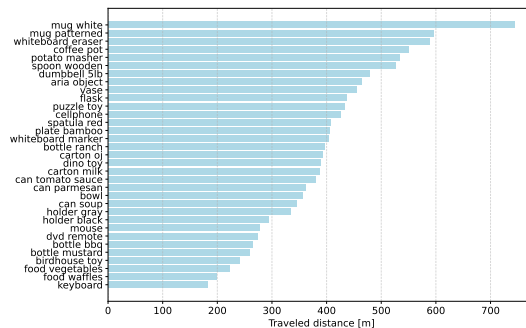


Figure 4. **Distances traveled by HOT3D objects.** In total, subjects moved the 33 objects over 13 km. While objects like the keyboard and waffles were mostly resting, the white mug is a true explorer.

formations from the 3D model space to the scene space, and hand poses are represented in the UmeTrack [26] and MANO [56] formats (UmeTrack is more accurate while MANO is more standard). Annotations in some frames may be missing or be of a lower quality. We visually inspected all recordings and flagged all frames with lower-quality poses. Out of 1.5M frames included in the dataset, 1.16M frames are fully annotated (*i.e.*, ground-truth poses of all hands and objects are available) and passed our inspection. We release all 1.5M frames, which may be useful for unsupervised training, and provide a mask of the valid frames. See Fig. 4 and the supplement for statistics of the ground-truth object poses.

**Training and test splits.** The training split of HOT3D includes recordings of 13 subjects (1M multi-view frames), and the test split includes recordings of the remaining 6 subjects (0.5M multi-view frames). Ground-truth pose annotations are publicly released only for the training split. Ground-truth annotations for the test split are accessible only by dedicated evaluation servers.

**Curated clips.** To facilitate benchmarking of various tracking and pose estimation methods, we also release 3832 curated clips





Figure 5. **Motion-capture lab.** The HOT3D dataset was collected using a motion-capture rig equipped with a few dozens of infrared exocentric OptiTrack cameras and light diffuser panels for illumination variability.

extracted from the full recordings. 2804 clips come from the training split and 1028 from the test split. Each clip has 150 frames (5 seconds) with ground-truth annotations available for all modeled objects and hands and passing our visual inspection.

**Object onboarding sequences.** To enable benchmarking model-free object tracking methods [62], which learn new objects from reference images, and 3D object reconstruction methods [42], HOT3D includes two types of onboarding sequences which show all possible views of each object: (1) sequences showing a static object on a desk, when the object is standing upright and upside-down, and (2) sequences showing an object manipulated by hands. The static onboarding setup is suitable for NeRF-like reconstruction methods [42], while the latter is more practical for AR/VR applications yet more challenging [22]. The ground-truth object poses are provided for all frames of the static sequences, but only for the first frame of the dynamic sequences. This is to simulate real-world settings, where the poses can be easily obtained by SfM [59] in the static setup, but are challenging to obtain in the dynamic setup. The ground-truth pose for the first frame of dynamic sequences is provided to define the canonical object space, which is necessary for evaluating 6DoF object tracking. Ground-truth hand poses are not provided for these sequences.

## 4. Experiments

Wearable headsets often feature multiple cameras, which naturally lends itself to the development of multi-view methods for 3D tasks. In this section, we demonstrate that multi-view methods outperform single-view methods for several popular egocentric tasks. First, we compare the single-view and multi-view versions of the UmeTrack [26] method for 3D hand tracking. Second, we extend the FoundPose [50] method for 6DoF pose estimation of unseen objects to multiple views and evaluate against the original version. Third, we develop a method for 3D lifting of unknown in-hand

objects by stereo matching of DINOv2 [49] features, which we compare against a single-view method similar to OSNOM [51].

### 4.1. 3D hand pose tracking

**Experimental setup.** The task is to estimate 3D locations of hand joints in every frame of given test sequences, with the ground-truth hand skeletons and 2D bounding boxes of visible hands provided. We train the UmeTrack [26] hand tracker on three variants of training data: (1) training sequences from the UmeTrack dataset, (2) HOT3D training sequences recorded with Quest 3, and (3) the combination of the two. The UmeTrack dataset was recorded with the Quest 2 headset, which has the same but differently arranged cameras compared to Quest 3, and includes 1397 real and 1397 synthetic sequences, each recorded at 30 fps for 15 seconds. The sequences depict single-hand motions and hand-hand interactions performed by 53 participants, but do not include any hand-object interactions. All three UmeTrack models were trained on two-view image streams with one of the views randomly masked out (as in [26]). The masking increases the tracking robustness and encourages the models not to rely on both views, which enables a fair comparison of their single- and two-view modes. We evaluate the models on all frames of test UmeTrack sequences and all frames of test HOT3D clips from Quest 3. The accuracy of the predicted 3D locations is measured by the Mean Keypoint Position Error (MPKE) [26].

**Results (Table 2).** When trained only on the UmeTrack dataset, the UmeTrack tracker performs poorly on HOT3D, especially on frames with hand-object interactions that are not present in the UmeTrack dataset (24.2 MKPE on HOT3D vs. 13.6 on UmeTrack in the single-view mode). Conversely, we see a similar accuracy drop on the UmeTrack dataset when the tracker is trained on HOT3D, mostly on frames with hand-hand interactions that are not present in HOT3D (23.7 MKPE on UmeTrack vs. 18.0 on HOT3D). The accuracy drop is even larger when the tracker is trained only on one of the datasets and evaluated on two-view sequences. This is because the datasets are recorded with different headsets (Quest 2 vs. Quest 3) and the tracker overfitted to the camera configuration seen at training time. The domain gap between the two datasets is effectively closed when the tracker is trained on both, achieving 13.4 MKPE on UmeTrack and 15.4 on HOT3D in the single-view mode. A significant 41% improvement (to 9.5 MKPE on UmeTrack and 10.9 on HOT3D) is then achieved when the model uses both views as input.

### 4.2. 6DoF pose estimation of unseen objects

**Experimental setup.** In this experiment we focus on the task of model-based 6DoF pose estimation (*i.e.*, 3D translation and 3D rotation) of unseen objects, which are learned during a short onboarding stage just from their CAD models [34]. We evaluate the original FoundPose [50], a recent open-source method that achieves the state-of-the-art results in refinement-free pose estimation from a single image, and its extension to multi-view input that we propose below. We evaluate coarse versions of these methods (without any pose refinement) on every 30th frame of the test HOT3D clips from both Aria and Quest 3. The methods are

Training dataset	Views	MKPE on	MKPE on
		UmeTrack ↓	HOT3D ↓
UmeTrack [26]	1	13.6	24.2
UmeTrack [26]	2	9.7	25.6
HOT3D-Quest3	1	23.7	18.0
HOT3D-Quest3	2	30.3	13.1
UmeTrack + HOT3D-Quest3	1	13.4	15.4
UmeTrack + HOT3D-Quest3	2	<b>9.5</b>	<b>10.9</b>

Table 2. **3D hand pose tracking by UmeTrack [26]**. Reported is the Mean Keypoint Position Error (MKPE, in mm) achieved on the UmeTrack and HOT3D-Quest3 datasets by single-view and two-view variants of the UmeTrack hand tracker, which was trained on training splits of either of the datasets or on their combination.

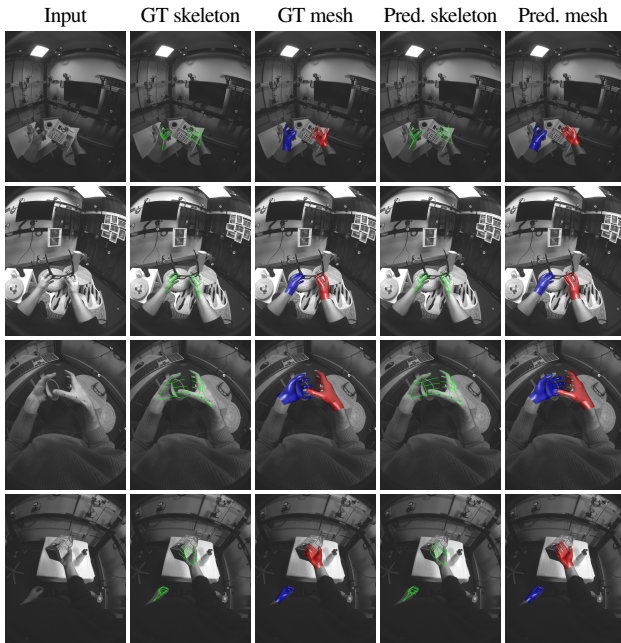


Figure 6. **Example 3D hand pose tracking results by UmeTrack [26]**. Shown are hand skeletons and meshes of the UmeTrack hand model in the ground-truth and estimated poses. The UmeTrack hand tracker was provided participant’s ground-truth hand skeleton and was tasked to estimate 3D locations of the skeleton joints.

provided ground-truth 2D segmentation masks of visible objects and are tasked to estimate the 6DoF object poses. The accuracy of the estimated poses is measured by a recall rate defined as the fraction of samples for which a correct pose was estimated. A pose estimate is considered correct if its symmetry-aware translational and rotational errors are below a threshold.

**FoundPose [50] and its multi-view extension.** During a short onboarding stage, FoundPose renders RGB-D templates showing the object model in different orientations, extracts DINOv2 patch features from the RGB channels, and registers the features in 3D using the depth channel. At inference time, FoundPose crops the

Test dataset	Views	Recall [%] ↑		
		5 cm, 5°	10 cm, 10°	20 cm, 20°
HOT3D-Aria	1	25.2	41.7	54.5
HOT3D-Aria	3	<b>33.8</b>	<b>52.9</b>	<b>66.2</b>
HOT3D-Quest3	1	28.9	46.6	58.9
HOT3D-Quest3	2	<b>36.9</b>	<b>55.9</b>	<b>66.4</b>

Table 3. **6DoF object pose estimation by FoundPose [50]**. The proposed multi-view extension of FoundPose is compared with the original single-view version in recall rates on test images from both headsets. The recall rate is defined as the fraction of pose estimates whose translational and rotational errors are below a specified threshold.

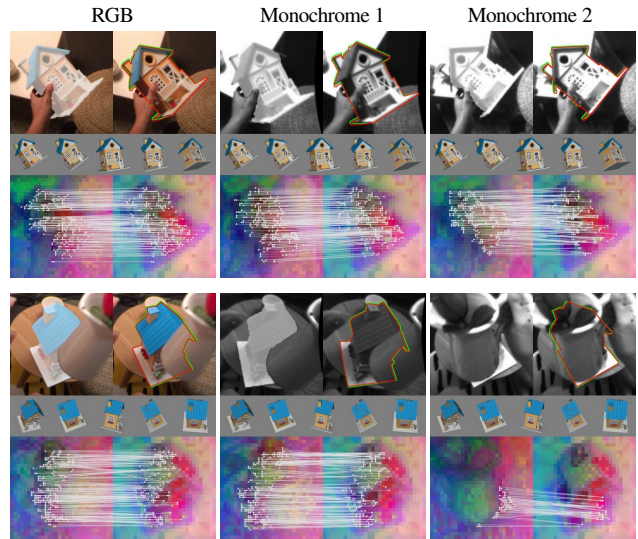


Figure 7. **Example 6DoF pose estimation results by FoundPose [50]**. Each row shows synchronized views of the same object from three Aria cameras. Our multi-view extension of FoundPose estimates the object pose from 2D-3D correspondences established between all available views and retrieved RGB-D templates. Thanks to the multi-view input, the method is able to estimate poses of heavily occluded objects (bottom row). Contours of 3D object models in the ground-truth and the estimated poses are shown in green and red respectively (top right corners). FoundPose was provided the ground-truth object mask as input (top left corners).

RGB query image around the object mask and retrieves a small set of most similar templates using a DINOv2-based bag-of-words approach. For each retrieved template, a pose hypothesis is generated by PnP-RANSAC from 2D-3D correspondences established by matching patch features of the image crop and the template. Finally, the pose hypothesis with the highest number of inlier correspondences is selected as the pose estimate.

To study the effect of multi- vs. single-view input for this task, we propose a straightforward multi-view extension of the original FoundPose method. The extended version relies on the same onboarding stage, but at inference time crops the object in all available views, retrieves a handful of templates with the highest sum of per-crop cosine similarities, establishes multi-view 2D-3D



correspondences between each of the templates and all views, and solves for the pose by solving the generalized  $PnP$  problem [37].

**Results (Table 3).** Our straightforward multi-view extension of FoundPose significantly outperforms the original single-view version, achieving 8–12% higher recall rates (13–34% relative improvement) on data from both headsets. Besides introducing additional constraints for 3D reasoning, the multi-view input offers more opportunities to observe objects that may be heavily or fully occluded in a single view. It is noteworthy that FoundPose performs well on the three-view setup from Aria, where one view is captured by a high-resolution RGB camera and the other two by lower-resolution monochrome cameras. We attribute this ability to generalize across different sensors primarily to DINOv2, which serves as the foundation model for FoundPose.

### 4.3. 2D segmentation of in-hand objects

**Experimental setup.** Given an input image, the task is to predict a binary 2D mask of objects manipulated by hands. Besides serving as a prerequisite for 3D lifting of in-hand objects (Sec. 4.4), this task is useful for downstream applications such as hand state classification or video activity recognition [75]. We evaluate three methods, including the off-the-shelf EgoHOS [75] and two variants of Mask R-CNN [28], trained on a proprietary dataset of 400K RGB Aria images annotated with 52K masks of in-hand objects. We trained one model directly on the RGB image channels (denoted as MRCNN in Tab. 4), and one on the depth channel predicted by Depth Anything V2 [72] (denoted as MRCNN-DA). We evaluate these methods on every 30th frame of the training and test HOT3D clips from both Aria and Quest3 (~19K frames). Objects are considered to be in-hand if the minimum distance between object and hand mesh vertices in their ground-truth poses is below a threshold of 1 cm and the object is moving with a velocity larger than 1 cm/s. Masks of such objects are used as the ground truth for this task. The accuracy of predicted masks is measured by mean Intersection over Union (mIoU), as in [75].

**Results (Table 4).** The EgoHOS [75] model exhibits a noticeable decline in accuracy on the HOT3D dataset compared to its performance on the EgoHOS dataset, which we attribute to the domain gap between the training datasets (different camera configurations/models). This is particularly evident in the ~50% lower accuracy on Quest 3 monochrome frames. MRCNN-DA is the top performing method, outperforming EgoHOS on Aria and Quest 3 frames by 30% and 65% respectively. The incorporation of predicted depth maps enables more accurate disambiguation of foreground in-hand objects from the background, resulting in improved segmentation masks (Fig. 8).

### 4.4. 3D lifting of in-hand objects

**Experimental setup.** Next we focus on the task of 3D lifting of unknown in-hand objects, which is useful for object indexing and long-term tracking [51]. Given per-view 2D segmentation masks of an in-hand object, the goal is to estimate the 3D object location in the camera coordinate frame. We developed and compare the performance of three methods described below. The accuracy

Method	Test dataset	Object in hand (mIoU $\uparrow$ ):			
		Either	Left	Right	Both
EgoHOS [75]	EgoHOS	–	62.2	44.4	52.8
EgoHOS [75]	HOT3D-Aria	42.6	21.0	26.3	32.5
MRCNN	HOT3D-Aria	47.1	–	–	–
MRCNN-DA	HOT3D-Aria	<b>55.2</b>	–	–	–
EgoHOS [75]	HOT3D-Quest3	33.1	13.5	14.4	24.8
MRCNN	HOT3D-Quest3	37.8	–	–	–
MRCNN-DA	HOT3D-Quest3	<b>54.7</b>	–	–	–

Table 4. **2D segmentation of in-hand objects.** EgoHOS [75] trained on the EgoHOS dataset is compared with our baselines based on Mask R-CNN [28] and trained on our in-house dataset of images from Aria. We observe a large accuracy drop of the EgoHOS model on HOT3D.

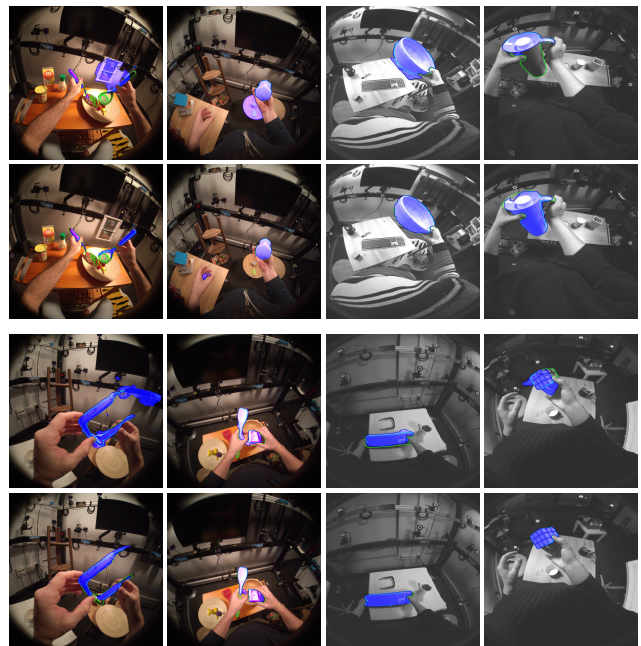


Figure 8. **Example results of 2D segmentation of in-hand objects.** Masks predicted by EgoHOS [75] (1st and 3rd row) are compared with masks predicted by our MRCNN-DA (2nd and 4th row). Predicted masks are shown in blue, and the contour of ground-truth masks in green.

of the estimated locations is measured by a recall rate defined as the fraction of samples for which a correct location was estimated. A location is considered correct if its offset from the ground-truth location, defined by the center of the 3D object bounding box, is below a threshold.

**Using hand as the object proxy (HandProxy).** As a simple baseline, we use the ground-truth 3D palm center as the object location. We calculate the palm center as the middle point between the wrist joint and the first joint of the middle finger. If both hands are visible, we use the 3D palm location whose 2D projection is closer to the 2D object mask centroid. The goal of this baseline is to evaluate whether a specialized solution is



Method	Test dataset	Views	Recall [%] $\uparrow$			
			5 cm	10 cm	20 cm	30 cm
HandProxy	HOT3D-Aria	–	0.5	13.5	90.6	98.4
Using ground-truth 2D segmentation masks:						
MonoDepth	HOT3D-Aria	1	14.3	30.2	53.6	69.9
StereoMatch	HOT3D-Aria	3	<b>64.4</b>	<b>86.2</b>	<b>95.5</b>	<b>96.9</b>
StereoMatch	HOT3D-Quest3	2	76.4	96.8	99.1	99.2
Using 2D segmentation masks predicted by MRCNN-DA:						
MonoDepth	HOT3D-Aria	1	11.1	23.3	43.7	58.2
StereoMatch	HOT3D-Aria	3	<b>42.6</b>	<b>56.4</b>	<b>63.6</b>	<b>66.0</b>
StereoMatch	HOT3D-Quest3	2	59.1	75.3	80.4	81.3

Table 5. **3D lifting of in-hand objects.** Shown are recall rates of our three baseline methods for several thresholds of correctness (a predicted 3D location is considered correct if its distance from the ground-truth location is below a threshold). The multi-view method (StereoMatch) clearly outperforms the other two methods at stricter threshold levels.

necessary for this task or whether an accurate 3D hand tracker could provide a sufficient estimate.

**Lifting by monocular depth estimation (MonoDepth).** Our second approach is inspired by [51] and relies on monocular depth prediction and sparse SLAM observations. Specifically, we predict a monocular depth map by applying Depth Anything V2 [72] to a rectilinear input image (warped from the fisheye camera to a pinhole camera), align it to the 3D point cloud from SLAM by a scale-shift transformation [51], and finally calculate the 3D object location as the median of the aligned depth values collected from the object mask. Since MonoDepth requires SLAM observations that are not available for Quest 3, we evaluate this method only on recordings from Aria (using RGB images).

**Lifting by stereo matching (StereoMatch).** Our third approach for 3D lifting of in-hand objects is based on matching DINOv2 features in stereo images. Given 2D object segmentation masks in two views, we first construct a stereo crop pair such as the crops closely surround the given masks, both have a resolution of  $420 \times 420$  pixels, and a pixel in one crop is guaranteed to have its corresponding pixel in the same pixel row of the other crop [4]. Next, we extract patch features from each of the crops using DINOv2 ViT-S [49], and establish 2D-2D correspondences between the crops by linking each patch from one crop with the nearest patch (in terms of L2 distance between DINOv2 feature vectors) from the same row in the other view. We retain upto 500 correspondences with the smallest cyclic distance [20], and triangulate them to obtain a set of 3D points. The 3D object location is estimated using the robust mean of the 3D point set.

**Results (Table 5)** The StereoMatch method outperforms the MonoDepth method on Aria recordings, regardless of whether the ground-truth segmentation masks or masks predicted by MRCNN-DA are used as input. The 3D localization error of MonoDepth is primarily oriented along the optical axis. This is evident in Fig. 9, where the localization error for the MonoDepth approach is most

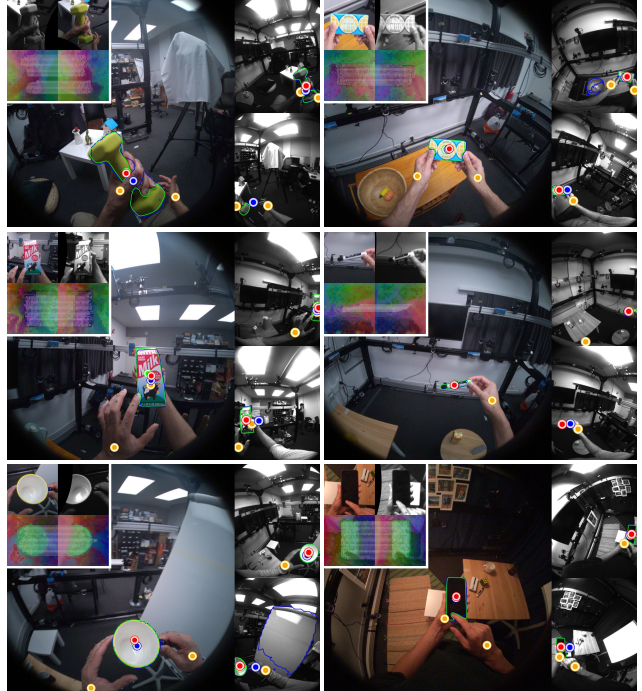


Figure 9. **Example results of 3D lifting of in-hand objects.** Ground-truth 3D object locations are shown in green, locations predicted by StereoMatch in red, by MonoDepth in blue, and by HandProxy in orange. The 3D locations are projected to the three views from Aria. In each sample, the RGB image is on the left and monochrome images on the right. The DINOv2 stereo matching between the RGB and one of the monochrome Aria images is visualized in the top left corners.

pronounced in camera viewpoints with a larger baseline w.r.t. the input RGB camera. Finally, the HandProxy baseline demonstrates that while hand tracking alone is sufficient for localizing objects within a 30 cm uncertainty radius (similar to evaluations in [51]), a dedicated method for multi-view 3D lifting of in-hand objects provides additional value for finer-grained localization within 10 cm.

## 5. Conclusion

We have introduced HOT3D, a large-scale, publicly available dataset designed to support training and evaluation of methods for various 2D and 3D egocentric tasks related to hand-object interaction. Our experiments show that multi-view methods, whose benchmarking is uniquely enabled by HOT3D, significantly outperform their single-view counterparts across several popular tasks. Besides multi-view 3D object tracking, we addressed the tasks of multi-view 6DoF pose estimation of unseen objects and 3D lifting of in-hand objects, for which we developed strong baselines. By publicly releasing the HOT3D dataset along with source code of the baseline methods, and by co-organizing public challenges<sup>1,2</sup> on the dataset, we hope to accelerate research on egocentric vision and contextual AI.

<sup>1</sup><https://bop.felk.cvut.cz/challenges/bop-challenge-2024/>

<sup>2</sup>[https://github.com/facebookresearch/hand\\_tracking\\_toolkit](https://github.com/facebookresearch/hand_tracking_toolkit)

**Acknowledgements.** Thanks to Ben Schneiders, Mateja Kodila, Elizabeth Béres, and Nicolas Greiner for organizing data collections and helping with data processing. Thanks to Fadime Sener, Bugra Tekin, Yann Labbé, Christian Forster, Mariano Jaimez, Rainer Stal, Timo Stoffregen, Pierluigi Taddei, Eric Sauser, Shitai Li, Lukas Bode, and Ben Schneiders for participating in the data collections. Thanks to Evgeniy Oleinik and Maien Hamed for help with hosting the dataset on Meta servers. Thanks to Xiaqing Pan for his guidance on open sourcing the HOT3D toolkit. Thanks to Mark Schwesinger, Christopher Pistrutto, Adam Szenderski, Elizabeth Argall, and Josiah Zacharias for providing legal and writing support to release HOT3D on time. Thanks to Nick Charron, Alexander Gamino, and David Caruso for their help with calibration and SLAM-OptiTrack alignment. Thanks to Ka Chen and Allison Tilp for supporting the creation of high-fidelity CAD models of the HOT3D objects. Thanks to Abha Arora, Luis Pesqueira, and Yuyang Zou for helping with organizing the Aria data campaign and setting up the Aria data collection infrastructure. Thanks to Tomasz Malisiewicz for his help with training models for 2D in-hand object segmentation.

## A. Aria glasses

Project Aria [13] is an egocentric recording device in glasses form-factor created by Meta. It is designed as a *research tool* for egocentric machine perception and contextualized AI research, and available to researchers across the world via [projectaria.com](https://projectaria.com).

### A.1. Device and sensors

Project Aria is built to emulate future AR- or smart-glasses catering to machine perception and egocentric AI rather than human consumption. It is designed to be wearable for long periods of time without obstructing or impeding the wearer, allowing for natural motion even when performing highly dynamic activities – such as playing soccer or dancing. It has a total weight of 75g (compared to over 150g for a single GoPro camera), and fits just like a pair of glasses.

Further, the device integrates a rich sensor suite that is tightly calibrated and time-synchronized, capturing a broad range of modalities. For HOT3D, *recording profile 15* is used, which uses the following sensor configuration (all streams come with meta-data such as precise timestamps and per-frame exposure times):

- **One rolling-shutter RGB camera** recording at 30 fps and  $1408 \times 1408$  resolution. It is fitted with an F-Theta fisheye lens that covers a field of view of  $110^\circ$ .
- **Two global-shutter monochrome cameras** recording at 30 fps and  $640 \times 480$  resolution. They provide additional peripheral vision, and are fitted with F-Theta fisheye lenses that cover a field of view of  $150^\circ$ .
- **Two monochrome eye-tracking cameras** recording at 10 fps and  $320 \times 240$  resolution.
- **Two IMUs** (800 Hz and 1000 Hz respectively), a **barometer** (50 fps) and a **magnetometer** (10 fps).
- **GNSS and WiFi** scanning was disabled for HOT3D.
- **Audio** recording was disabled for HOT3D for privacy reasons.



Figure 10. Project Aria research glasses.

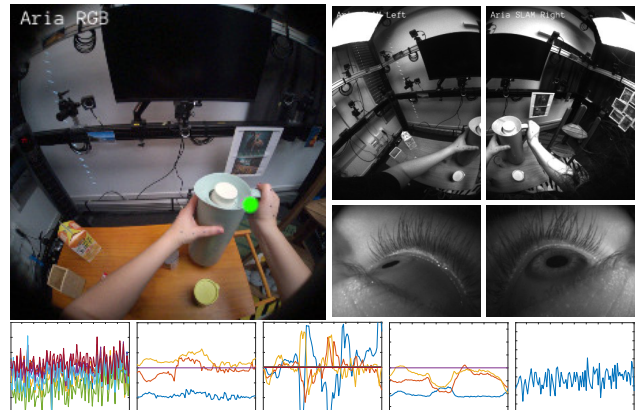


Figure 11. Sensor streams recorded by the Project Aria device. Top: RGB camera, left and right monochrome and eye cameras. Bottom: 10-second extracts from microphones, accelerometer, gyroscope, magnetometer and barometer respectively.

### A.2. Machine Perception Services (MPS)

Project Aria’s machine perception service (MPS) provides software building blocks that simplify leveraging the different modalities recorded. These functionalities are likely to be available as real-time, on-device capabilities in future AR- or smart-glasses. We use the following core functionalities currently offered by Project Aria, and include their raw output as part of the dataset. See [13] and the technical documentation<sup>3</sup> for more details.

**Calibration.** All sensors are intrinsically and extrinsically calibrated, and tiny deformations due to temperature changes or stress applied to the glasses frame are further corrected by time-varying online calibration from MPS.

**Aria 6 DoF localization.** Every recording is localized precisely and robustly in a common, metric, gravity-aligned coordinate frame, using a state-of-the-art VIO and SLAM algorithm. This provides millimeter-accurate 6DoF poses for every captured frame and high-frequency (1 kHz) motion in-between frames.

**Eye gaze.** The gaze direction of the user is estimated as two outward-facing rays anchored approximately at the wearer’s eyes, allowing to approximately estimate not only the direction the user is looking in, but also the depth their eyes are focused on. We use an optional eye gaze calibration procedure, where the mobile companion app directs the wearer to gaze at a pattern

<sup>3</sup>[https://facebookresearch.github.io/projectaria\\_tools/docs/intro](https://facebookresearch.github.io/projectaria_tools/docs/intro)



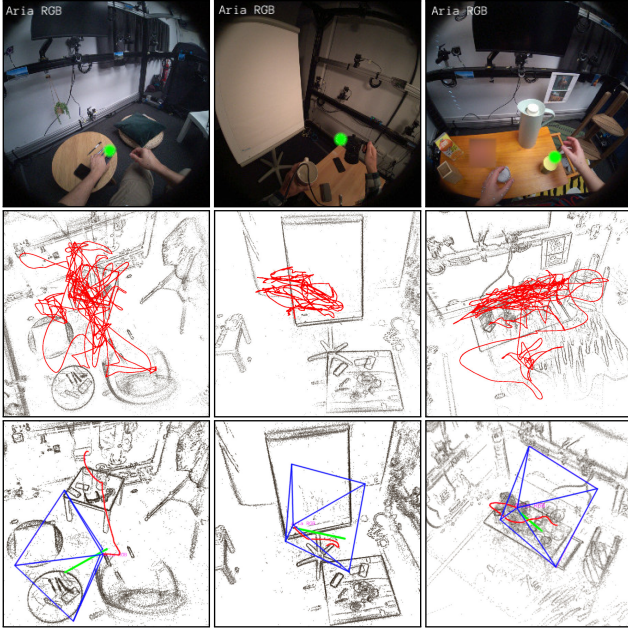


Figure 12. **Aria MPS output.** Shown is output for three recordings in a living room, office and kitchen scenario respectively (left to right). Top: RGB view and gaze (green dot). Middle: Point cloud and estimated egocentric camera trajectory for the full recording. Bottom: 3D view of a specific point in time, showing the RGB camera frustum (blue), gaze vector (green) and trajectory from the previous second (red).

on the phone screen while performing specific head movements. This information was then used to generate a more accurate eye gaze direction, personalized to the particular wearer.

**Point clouds.** A 3D point cloud of static scene elements is triangulated from the moving Aria device, using photometric stereo over consecutive frames or left/right SLAM camera. Points are added causally over time, and will include points on any object that is observed while static for several seconds. The output contains both the 3D point clouds as well as the raw 2D observations of every point in the camera images it was triangulated from.

### A.3. Processing summary

All Aria recordings are anonymized in a very first step, using the public EgoBlur [53] model and following Project Aria’s responsible innovation principles.

Then, the MPS pipeline is invoked for each full Aria recording, which are typically about 2 minutes long and include many instances of hand-object interactions with different objects. Next, we 7DoF-align the MPS output with the OptiTrack coordinate frame (App. C). In total, we have processed 199 Aria recordings with a total length of 391 minutes.

### A.4. Tools and ecosystem

Documentation and open-source tooling for Aria recordings and MPS output is available on GitHub<sup>4</sup> and includes Python and

<sup>4</sup>[https://github.com/facebookresearch/projectaria\\_tools](https://github.com/facebookresearch/projectaria_tools)



Figure 13. **Meta Quest 3 headset for virtual and mixed reality.**



Figure 14. **Sample images from Quest 3.** Shown are synchronized images from the two front Quest 3 cameras used for the HOT3D collection.

C++ tools to convert, load, and visualize data, as well as sample code for common computer vision tasks.

## B. Quest 3 headset

Quest 3 [41], shown in Fig. 13, is the latest production headset from Meta for virtual- and mixed-reality experiences. For the HOT3D data collection we used a developer version of the Quest 3 headset. This version has four global-shutter monochrome cameras with fisheye lenses, 1280x1024 px image resolution, 18 PPD (Pixels Per Degree), and records at 30 fps. Two of the cameras are on the front side of the headset, roughly aligned with eyes, and two on the sides. HOT3D only includes images from the two front cameras as those capture the relevant scene part (the two side cameras are useful for applications like SLAM). Example images are in Fig. 14. Data from other sensors present in the consumer version of Quest 3, including a gyroscope and an accelerometer, were not recorded. The intrinsic and extrinsic parameters of the headset cameras were calibrated with a ChArUco board. Both the headset and the board were attached a set of optical markers and tracked by the motion-capture system described in App. C, which allowed to estimate camera-to-headset transformations. At recording time, the headset pose was still tracked by the motion-capture system and used to calculate per-frame camera-to-world transformations.

## C. Marker-based motion capture

The poses of hands and objects were tracked using optical markers attached on their surface. For both hands and objects we used 3 mm markers with an adhesive layer at their bottom. Such markers are small enough not to influence hand-object interactions. Each hand was attached 19 markers and each object around 10. The marker locations were then semi-automatically registered to



Method	Test dataset	Object in hand (mIoU $\uparrow$ ) for training + test / training / test split:			
		Either	Left	Right	Both
EgoHOS [75]	EgoHOS	–	62.2	44.4	52.8
EgoHOS [75]	HOT3D-Aria	42.6 / 43.5 / 40.1	21.0 / 21.0 / 21.3	26.3 / 25.8 / 28.2	32.5 / 33.0 / 30.5
MRCNN	HOT3D-Aria	47.1 / 48.1 / 43.7	–	–	–
MRCNN-DA	HOT3D-Aria	<b>55.2 / 56.3 / 51.6</b>	–	–	–
EgoHOS [75]	HOT3D-Quest3	33.1 / 33.8 / 31.4	13.5 / 12.9 / 15.0	14.4 / 13.9 / 15.6	24.8 / 25.6 / 22.9
MRCNN	HOT3D-Quest3	37.8 / 38.2 / 36.9	–	–	–
MRCNN-DA	HOT3D-Quest3	<b>54.7 / 54.7 / 54.8</b>	–	–	–

Table 6. **2D segmentation of in-hand objects.** Each cell shows the mIoU score achieved on the training + test, training, and test split, respectively.

Method	Test dataset	Views	Recall [%] $\uparrow$ for training + test / training / test split:			
			5 cm	10 cm	20 cm	30 cm
HandProxy	HOT3D-Aria	–	0.5 / 0.5 / 0.6	13.5 / 11.6 / 20.2	90.6 / 89.9 / 93.3	98.4 / 98.0 / 99.3
Using ground-truth 2D segmentation masks:						
MonoDepth	HOT3D-Aria	1	14.3 / 13.4 / 17.5	30.2 / 28.8 / 34.8	53.6 / 51.7 / 60.4	69.9 / 68.2 / 76.0
StereoMatch	HOT3D-Aria	3	<b>64.4 / 65.0 / 62.6</b>	<b>86.2 / 86.3 / 86.0</b>	<b>95.5 / 95.1 / 96.8</b>	<b>96.9 / 96.6 / 98.3</b>
StereoMatch	HOT3D-Quest3	2	76.4 / 78.0 / 72.8	96.8 / 96.9 / 96.5	99.1 / 99.2 / 99.1	99.2 / 99.2 / 99.1
Using 2D segmentation masks predicted by MRCNN-DA:						
MonoDepth	HOT3D-Aria	1	11.1 / 10.6 / 12.7	23.3 / 22.4 / 26.5	43.7 / 42.6 / 47.5	58.2 / 57.5 / 60.8
StereoMatch	HOT3D-Aria	3	<b>42.6 / 43.9 / 38.4</b>	<b>56.4 / 57.6 / 52.2</b>	<b>63.6 / 64.9 / 59.1</b>	<b>66.0 / 67.4 / 61.2</b>
StereoMatch	HOT3D-Quest3	2	59.1 / 60.1 / 56.9	75.3 / 75.6 / 74.6	80.4 / 80.6 / 79.9	81.3 / 81.6 / 80.7

Table 7. **3D lifting of in-hand objects.** Each cell shows the recall rate achieved on the training + test, training, and test split, respectively.

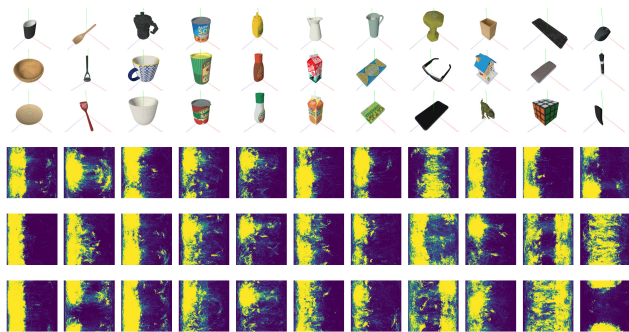


Figure 15. **Object orientation statistics.** Top: 3D object models in their canonical poses. Bottom: Distribution of azimuth and elevation angles under which the objects are observed across the dataset. The vertical axis is the azimuth angle  $[0^\circ, 360^\circ]$  (angle along the green axis), and the horizontal axis is the elevation angle  $[-90^\circ, 90^\circ]$  (angle w.r.t. the plane defined by the red and blue axes).

3D models of hands and objects obtained by custom 3D scanners.

At recording time, the optical markers were tracked by multiple infrared OptiTrack cameras attached on a rig shown in Fig. 5 of the main paper. The intrinsic and extrinsic parameters of the infrared cameras were calibrated before every capturing session. Hand poses were calculated by fitting the participant’s UmeTrack hand model [26] to the tracked optical markers, as in [25]. Object

poses were estimated by aligning the tracked markers to their registered 3D locations in the model coordinate frame. To achieve reliable tracking, it was important to ensure that the marker constellation on each object is sufficiently distinct. Data frames from different sources were synchronized with SMPTE timecode.

#### D. Object orientation statistics

When recording HOT3D, we asked subjects to naturally interact with the objects. Consequently, orientation distributions of the observed objects (Fig. 15) reveal clear object-specific pose biases, which may be useful as prior information at inference time (we see that the bowl tends to be seen upright, the birdhouse from the front and upright, *etc.*).

#### E. Additional quantitative results

The results of 2D segmentation and 3D lifting of in-hand objects presented in Tables 4 and 5 were obtained by evaluating methods on clips from both training and test splits. To allow the community to compare their results against our results on these two tasks, we additionally provide results obtained on clips from the training split for which the ground-truth annotations are publicly available (Tables 6 and 7). Evaluating on the training split is possible as both of these tasks are training-free and therefore do not require any training split.

## References

- [1] Sven Bambach, Stefan Lee, David J. Crandall, and Chen Yu. Lending a hand: Detecting hands and recognizing activities in complex egocentric interactions. In *ICCV*, 2015. [3](#)
- [2] Ameline Bardo, Katie Town, Tracy L Kivell, Georgina Donati, Haiko Ballieux, Cosmin Stamate, Trudi Edginton, and Gillian S Forrester. The precision of the human hand: variability in pinch strength and manual dexterity. *Symmetry*, 2022. [1](#)
- [3] Bharat Lal Bhatnagar, Xianghui Xie, Ilya Petrov, Cristian Sminchisescu, Christian Theobalt, and Gerard Pons-Moll. BEHAVE: Dataset and method for tracking human object interactions. In *CVPR*, 2022. [3](#)
- [4] Gary Bradski. Learning OpenCV: Computer vision with the OpenCV library. *O'REILLY*, 2008. [8](#)
- [5] Samarth Brahmabhatt, Catherine Ham, Charles C Kemp, and James Hays. ContactPose: A dataset of grasps with object contact and hand pose. In *ECCV*, 2020. [3, 4](#)
- [6] Ian M. Bullock, Thomas Feix, and Aaron M. Dollar. The Yale human grasping dataset: Grasp, object, and task data in household and machine shop environments. *IJRR*, 2015. [3](#)
- [7] Berk Calli, Arjun Singh, Aaron Walsman, Siddhartha Srinivasa, Pieter Abbeel, and Aaron M Dollar. The YCV object and model set: Towards common benchmarks for manipulation research. In *ICAR*, 2015. [3](#)
- [8] Yu-Wei Chao, Wei Yang, Yu Xiang, Pavlo Molchanov, Ankur Handa, Jonathan Tremblay, Yashraj S. Narang, Karl Van Wyk, Umar Iqbal, Stan Birchfield, Jan Kautz, and Dieter Fox. DexYCB: A benchmark for capturing hand grasping of objects. In *CVPR*, 2021. [3](#)
- [9] Woojin Cho, Jihyun Lee, Minjae Yi, Minje Kim, Taeyun Woo, Donghwan Kim, Taewook Ha, Hyekeun Lee, Je-Hwan Ryu, Woon-tack Woo, and Tae-Kyun Kim. Dense hand-object(ho) graspnet with full grasping taxonomy and dynamics. In *ECCV*, 2024. [3](#)
- [10] Dima Damen, Hazel Doughty, Giovanni Maria Farinella, Antonino Furnari, Jian Ma, Evangelos Kazakos, Davide Moltisanti, Jonathan Munro, Toby Perrett, Will Price, and Michael Wray. Rescaling egocentric vision: Collection, pipeline and challenges for EPIC-KITCHENS-100. *IJCV*, 2022. [3](#)
- [11] Maximilian Denninger, Martin Sundermeyer, Dominik Winkelbauer, Dmitry Olefir, Tomáš Hodaň, Youssef Zidan, Mohamad Elbadrawy, Markus Knauer, Harinandan Katam, and Ahsan Lodhi. BlenderProc: Reducing the reality gap with photorealistic rendering. *RSS Workshops*, 2020. [3](#)
- [12] Maximilian Denninger, Martin Sundermeyer, Dominik Winkelbauer, Youssef Zidan, Dmitry Olefir, Mohamad Elbadrawy, Ahsan Lodhi, and Harinandan Katam. Blenderproc. *arXiv preprint arXiv:1911.01911*, 2019. [3](#)
- [13] Jakob Engel, Kiran Somasundaram, Michael Goesele, Albert Sun, Alexander Gamino, Andrew Turner, Arjang Talattof, Arnie Yuan, Bilal Souti, Brighid Meredith, Cheng Peng, Chris Sweeney, Cole Wilson, Dan Barnes, Daniel DeTone, David Caruso, Derek Valleroy, Dinesh Ginjupalli, Duncan Frost, Edward Miller, Elias Mueggler, Evgeniy Oleinik, Fan Zhang, Guruprasad Somasundaram, Gustavo Solaira, Harry Lanaras, Henry Howard-Jenkins, Huixuan Tang, Hyo Jin Kim, Jaime Rivera, Ji Luo, Jing Dong, Julian Straub, Kevin Bailey, Kevin Eickenhoff, Lingni Ma, Luis Pesqueira, Mark Schwesinger, Maurizio Monge, Nan Yang, Nick Charron, Nikhil Raina, Omkar Parkhi, Peter Borschowa, Pierre Moulon, Prince Gupta, Raul Mur-Artal, Robbie Pennington, Sachin Kulkarni, Sagar Miglani, Santosh Gondi, Saransh Solanki, Sean Diener, Shangyi Cheng, Simon Green, Steve Saarinen, Suvam Patra, Tassos Mourikis, Thomas Whelan, Tripti Singh, Vasileios Balntas, Vijay Baiyya, Wilson Dreeves, Xiaqing Pan, Yang Lou, Yipu Zhao, Yusuf Mansour, Yuyang Zou, Zhaoyang Lv, Zijian Wang, Mingfei Yan, Carl Ren, Renzo De Nardi, and Richard Newcombe. Project Aria: A new tool for egocentric multi-modal AI research, 2023. [1, 2, 3, 4, 9](#)
- [14] Mark Everingham, Luc Van Gool, Christopher KI Williams, John Winn, and Andrew Zisserman. The PASCAL visual object classes (VOC) challenge. *IJCV*, 2010. [3](#)
- [15] Zicong Fan, Omid Taheri, Dimitrios Tzionas, Muhammed Kocabas, Manuel Kaufmann, Michael J Black, and Otmar Hilliges. ARCTIC: A dataset for dexterous bimanual hand-object manipulation. In *CVPR*, 2023. [3, 4](#)
- [16] Alireza Fathi, Xiaofeng Ren, and James M. Rehg. Learning to recognize objects in egocentric activities. In *CVPR*, 2011. [3](#)
- [17] Yang Fu and Xiaolong Wang. Category-level 6D object pose estimation in the wild: A semi-supervised learning approach and a new dataset. *NeurIPS*, 2022. [3](#)
- [18] Guillermo Garcia-Hernando, Shanxin Yuan, Seungryul Baek, and Tae-Kyun Kim. First-person hand action benchmark with RGB-D videos and 3D hand pose annotations. In *CVPR*, 2018. [3](#)
- [19] Andreas Geiger, Philip Lenz, and Raquel Urtasun. Are we ready for autonomous driving? The KITTI vision benchmark suite. In *CVPR*, 2012. [3](#)
- [20] Walter Goodwin, Sagar Vaze, Ioannis Havoutis, and Ingmar Posner. Zero-shot category-level object pose estimation. In *ECCV*, 2022. [8](#)
- [21] Andrew Guo, Bowen Wen, Jianhe Yuan, Jonathan Tremblay, Stephen Tyree, Jeffrey Smith, and Stan Birchfield. HANDAL: A dataset of real-world manipulable object categories with pose annotations, affordances, and reconstructions. In *IROS*, 2023. [3](#)
- [22] Shreyas Hampali, Tomas Hodan, Luan Tran, Lingni Ma, Cem Keskin, and Vincent Lepetit. In-hand 3D object scanning from an RGB sequence. In *CVPR*, 2023. [5](#)
- [23] Shreyas Hampali, Mahdi Rad, Markus Oberweger, and Vincent Lepetit. HONnotate: A method for 3D annotation of hand and object poses. In *CVPR*, pages 3196–3206, 2020. [3](#)
- [24] Shreyas Hampali, Sayan Deb Sarkar, Mahdi Rad, and Vincent Lepetit. Keypoint transformer: Solving joint identification in challenging hands and object interactions for accurate 3D pose estimation. In *CVPR*, 2022. [3](#)
- [25] Shangchen Han, Beibei Liu, Robert Wang, Yuting Ye, Christopher D. Twigg, and Kenrick Kin. Online optical marker-based hand tracking with deep labels. *ACM Trans. Graph.*, 37(4):166:1–166:10, July 2018. [11](#)
- [26] Shangchen Han, Po-chen Wu, Yubo Zhang, Beibei Liu, Linguang Zhang, Zheng Wang, Weiguang Si, Peizhao Zhang, Yujun Cai, Tomas Hodan, et al. UmeTrack: Unified multi-view end-to-end hand tracking for VR. In *SIGGRAPH Asia 2022*, 2022. [3, 4, 5, 6, 11](#)
- [27] Yana Hasson, Gül Varol, Dimitrios Tzionas, Igor Kalevtykh, Michael J Black, Ivan Laptev, and Cordelia Schmid. Learning joint reconstruction of hands and manipulated objects. In *CVPR*, 2019. [3](#)
- [28] Kaiming He, Georgia Gkioxari, Piotr Dollár, and Ross Girshick. Mask R-CNN. *ICCV*, 2017. [7](#)
- [29] Tony Heap and David Hogg. Towards 3D hand tracking using a deformable model. In *Proceedings of the Second International Conference on Automatic Face and Gesture Recognition*, 1996. [3](#)

- [30] Stefan Hinterstoisser, Vincent Lepetit, Slobodan Ilic, Stefan Holzer, Gary Bradski, Kurt Konolige, and Nassir Navab. Model based training, detection and pose estimation of texture-less 3D objects in heavily cluttered scenes. In *ACCV*, 2013. 3
- [31] Tomáš Hodaň, Pavel Haluza, Štěpán Obdržálek, Jiří Matas, Manolis Lourakis, and Xenophon Zabulis. T-LESS: An RGB-D dataset for 6D pose estimation of texture-less objects. *WACV*, 2017. 3
- [32] Tomáš Hodaň, Frank Michel, Eric Brachmann, Wadim Kehl, Anders Glent Buch, Dirk Kraft, Bertram Drost, Joel Vidal, Stephan Ihrke, Xenophon Zabulis, Caner Sahin, Fabian Manhardt, Federico Tombari, Tae-Kyun Kim, Jiří Matas, and Carsten Rother. BOP: Benchmark for 6D object pose estimation. *ECCV*, 2018. 3
- [33] Tomáš Hodaň, Martin Sundermeyer, Bertram Drost, Yann Labbé, Eric Brachmann, Frank Michel, Carsten Rother, and Jiří Matas. BOP Challenge 2020 on 6D object localization. In *ECCV*, 2020. 3, 4
- [34] Tomáš Hodaň, Martin Sundermeyer, Yann Labbé, Van Nguyen Nguyen, Gu Wang, Eric Brachmann, Bertram Drost, Vincent Lepetit, Carsten Rother, and Jiří Matas. BOP challenge 2023 on detection, segmentation and pose estimation of seen and unseen rigid objects. *CVPRW*, 2024. 3, 5
- [35] Tomáš Hodaň, Vibhav Vineet, Ran Gal, Emanuel Shalev, Jon Hanzelka, Treb Connell, Pedro Urbina, Sudipta Sinha, and Brian Guenter. Photorealistic image synthesis for object instance detection. *ICIP*, 2019. 4
- [36] HyunJun Jung, Guangyao Zhai, Shun-Cheng Wu, Patrick Ruhkamp, Hannah Schieber, Giulia Rizzoli, Pengyuan Wang, Hongcheng Zhao, Lorenzo Garattoni, Sven Meier, et al. House-Cat6D – a large-scale multi-modal category level 6D object perception dataset with household objects in realistic scenarios. *arXiv preprint arXiv:2212.10428*, 2022. 3
- [37] Zuzana Kukelova, Jan Heller, and Andrew Fitzgibbon. Efficient intersection of three quadrics and applications in computer vision. In *CVPR*, 2016. 7
- [38] Taein Kwon, Bugra Tekin, Jan Stuhmer, Federica Bogo, and Marc Pollefeys. H2O: A benchmark for egocentric hand-object interaction recognition. *IEEE Transactions on Multimedia*, 2020. 3
- [39] Yunze Liu, Yun Liu, Che Jiang, Kangbo Lyu, Weikang Wan, Hao Shen, Boqiang Liang, Zhoujie Fu, He Wang, and Li Yi. HOI4D: A 4D egocentric dataset for category-level human-object interaction. In *CVPR*, 2022. 3
- [40] Wes McDermott. *The PBR guide*. Allegorithmic, 2018. 2, 4
- [41] Meta. Quest 3. <https://www.meta.com/quest/quest-3/>, 2023. 1, 2, 4, 10
- [42] Ben Mildenhall, Pratul P Srinivasan, Matthew Tancik, Jonathan T Barron, Ravi Ramamoorthi, and Ren Ng. NeRF: Representing scenes as neural radiance fields for view synthesis. *ECCV*, 2020. 5
- [43] Gyeongsik Moon, Shouo-I Yu, He Wen, Takaaki Shiratori, and Kyoung Mu Lee. Interhand2.6M: A dataset and baseline for 3D interacting hand pose estimation from a single RGB image. In *ECCV*, 2020. 3
- [44] Franziska Mueller, Dushyant Mehta, Oleksandr Sotnychenko, Srinath Sridhar, Dan Casas, and Christian Theobalt. Real-time hand tracking under occlusion from an egocentric RGB-D sensor. In *ICCV*, 2017. 3
- [45] Hiroshi Murase and Shree K Nayar. Visual learning and recognition of 3-D objects from appearance. *IJCV*, 1995. 3
- [46] Richard A Newcombe, Shahram Izadi, Otmar Hilliges, David Molyneaux, David Kim, Andrew J Davison, Pushmeet Kohi, Jamie Shotton, Steve Hodges, and Andrew Fitzgibbon. KinectFusion: Real-time dense surface mapping and tracking. *ISMAR*, 2011. 3
- [47] Takehiko Ohkawa, Kun He, Fadime Sener, Tomas Hodan, Luan Tran, and Cem Keskin. AssemblyHands: Towards egocentric activity understanding via 3D hand pose estimation. In *CVPR*, 2023. 3
- [48] Iason Oikonomidis, Guillermo Garcia-Hernando, Angela Yao, Antonis Argyros, Vincent Lepetit, and Tae-Kyun Kim. HANDS18: Methods, techniques and applications for hand observation. In *ECCVW*, 2018. 1
- [49] Maxime Oquab, Timothée Darcet, Théo Moutakanni, Huy Vo, Marc Szafraniec, Vasil Khalidov, Pierre Fernandez, Daniel Haziza, Francisco Massa, Alaaeldin El-Nouby, et al. DINOv2: Learning robust visual features without supervision. *arXiv preprint arXiv:2304.07193*, 2023. 2, 5, 8
- [50] Evin Pinar Örnek, Yann Labbé, Bugra Tekin, Lingni Ma, Cem Keskin, Christian Forster, and Tomas Hodan. FoundPose: Unseen object pose estimation with foundation features. *ECCV*, 2024. 2, 5, 6
- [51] Chiara Plizzari, Shubham Goel, Toby Perrett, Jacob Chalk, Angjoo Kanazawa, and Dima Damen. Spatial cognition from egocentric video: Out of sight, not out of mind. *arXiv preprint arXiv:2404.05072*, 2024. 2, 5, 7, 8
- [52] Francesco Ragusa, Rosario Leonardi, Michele Mazzamuto, Claudia Bonanno, Rosario Scavo, Antonino Furnari, and Giovanni Maria Farinella. Enigma-51: Towards a fine-grained understanding of human-object interactions in industrial scenarios. *IEEE Winter Conference on Application of Computer Vision (WACV)*, 2024. 3
- [53] Nikhil Raina, Guruprasad Somasundaram, Kang Zheng, Sagar Miglani, Steve Saarinen, Jeff Meissner, Mark Schwesinger, Luis Pesqueira, Ishita Prasad, Edward Miller, Prince Gupta, Mingfei Yan, Richard Newcombe, Carl Ren, and Omkar M Parkhi. EgoBlur: Responsible innovation in Aria, 2023. 10
- [54] James M Rehg and Takeo Kanade. Visual tracking of high DoF articulated structures: an application to human hand tracking. In *ECCV*, 1994. 3
- [55] Lawrence G Roberts. *Machine perception of three-dimensional solids*. PhD thesis, Massachusetts Institute of Technology, 1963. 3
- [56] Javier Romero, Dimitrios Tzionas, and Michael J Black. Embodied hands: Modeling and capturing hands and bodies together. *TOG*, 2017. 4
- [57] Olga Russakovsky, Jia Deng, Hao Su, Jonathan Krause, Sanjeev Satheesh, Sean Ma, Zhiheng Huang, Andrej Karpathy, Aditya Khosla, Michael Bernstein, et al. Imagenet large scale visual recognition challenge. *IJCV*, 2015. 3
- [58] Daniel Scharstein and Richard Szeliski. A taxonomy and evaluation of dense two-frame stereo correspondence algorithms. *IJCV*, 2002. 3
- [59] Johannes L Schonberger and Jan-Michael Frahm. Structure-from-motion revisited. In *CVPR*, 2016. 5
- [60] Dandan Shan, Jiaqi Geng, Michelle Shu, and David F Fouhey. Understanding human hands in contact at internet scale. In *CVPR*, 2020. 3
- [61] Srinath Sridhar, Franziska Mueller, Michael Zollhöfer, Dan Casas, Antti Oulasvirta, and Christian Theobalt. Real-time joint tracking of a hand manipulating an object from RGB-D input. In *ECCV*, 2016. 3
- [62] Jiaming Sun, Zihao Wang, Siyu Zhang, Xingyi He, Hongcheng Zhao, Guofeng Zhang, and Xiaowei Zhou. OnePose: One-shot object pose estimation without cad models. In *CVPR*, 2022. 3, 5
- [63] Xiao Sun, Yichen Wei, Shuang Liang, Xiaou Tang, and Jian Sun. Cascaded hand pose regression. In *CVPR*, 2015. 3



- [64] Martin Sundermeyer, Tomas Hodan, Yann Labbé, Gu Wang, Eric Brachmann, Bertram Drost, Carsten Rother, and Jiri Matas. BOP challenge 2022 on detection, segmentation and pose estimation of specific rigid objects. *CVPRW*, 2023. 3
- [65] Danhang Tang, Hyung Jin Chang, Alykhan Tejani, and Tae-Kyun Kim. Latent regression forest: Structured estimation of 3D articulated hand posture. In *CVPR*, 2014. 3
- [66] Jonathan Tompson, Murphy Stein, Yann Lecun, and Ken Perlin. Real-time continuous pose recovery of human hands using convolutional networks. *ToG*, 2014. 3
- [67] Dimitrios Tzionas, Luca Ballan, Abhilash Srikantha, Pablo Aponte, Marc Pollefeys, and Juergen Gall. Capturing hands in action using discriminative salient points and physics simulation. *IJCV*, 2016. 3
- [68] Dorin Ungureanu, Federica Bogo, Silvano Galliani, Pooja Sama, Xin Duan, Casey Meekhof, Jan Stühmer, Thomas J Cashman, Bugra Tekin, Johannes L Schönberger, et al. Hololens 2 research mode as a tool for computer vision research. *arXiv*, 2020. 3
- [69] Jikai Wang, Qifan Zhang, Yu-Wei Chao, Bowen Wen, Xiaohu Guo, and Yu Xiang. Ho-cap: A capture system and dataset for 3d reconstruction and pose tracking of hand-object interaction, 2024. 3
- [70] Pengyuan Wang, HyunJun Jung, Yitong Li, Siyuan Shen, Rahul Parthasarathy Srikanth, Lorenzo Garattoni, Sven Meier, Nasir Navab, and Benjamin Busam. Phocal: A multi-modal dataset for category-level object pose estimation with photometrically challenging objects. In *CVPR*, 2022. 3
- [71] Yu Xiang, Tanner Schmidt, Venkatraman Narayanan, and Dieter Fox. PoseCNN: A convolutional neural network for 6D object pose estimation in cluttered scenes. *RSS*, 2018. 3
- [72] Lihe Yang, Bingyi Kang, Zilong Huang, Zhen Zhao, Xiaogang Xu, Jiashi Feng, and Hengshuang Zhao. Depth anything v2. *arXiv:2406.09414*, 2024. 7, 8
- [73] Shanxin Yuan, Qi Ye, Guillermo Garcia-Hernando, and Tae-Kyun Kim. The 2017 HANDS in the million challenge on 3D hand pose estimation. *arXiv preprint arXiv:1707.02237*, 2017. 3
- [74] Jiawei Zhang, Jianbo Jiao, Mingliang Chen, Liangqiong Qu, Xiaobin Xu, and Qingxiong Yang. 3D hand pose tracking and estimation using stereo matching. *arXiv preprint arXiv:1610.07214*, 2016. 3
- [75] Lingzhi Zhang, Shenghao Zhou, Simon Stent, and Jianbo Shi. Fine-grained egocentric hand-object segmentation: Dataset, model, and applications. In *ECCV*, 2022. 3, 7, 11
- [76] Christian Zimmermann, Duygu Ceylan, Jimei Yang, Bryan Russell, Max Argus, and Thomas Brox. FreiHAND: A dataset for markerless capture of hand pose and shape from single RGB images. In *ICCV*, 2019. 3